



SAPIENZA
UNIVERSITÀ DI ROMA

Spectral and Spatial Tailoring of Second Harmonic Generation in coupled Plasmonic Nanoantennas.

M. Centini

**Dipartimento di Scienze di Base ed Applicate per l'Ingegneria (SBAI),
Sapienza, Università di Roma,
via A. Scarpa 16, 00161, Roma (Italy)**

NanoInnovation 2016, 20-23 September, Roma.

OUTLINE

Enhancement of Second harmonic generation by surface plasmon polariton excitation;

Nonlinear response of metals; Integration method.

Second harmonic generation from dipole nanoantennas:

bulk and surface contributions separately investigated by geometry induced selective enhancement.

Second harmonic generation from coupled metal nanorods:

engineering the near field and far field emission patterns;

Conclusions.

Nonlinear frequency conversion at the nanoscale: Main features

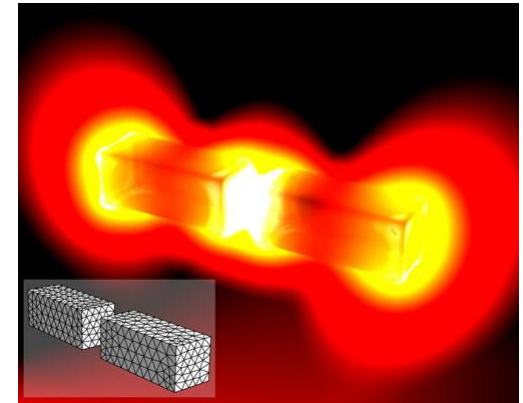
A) phase mismatch does not play a crucial role:

- the field is confined and localized in subwavelength regions

B) Field localization at the fundamental frequency field and at the second harmonic field is important

- Optimal conditions are achieved if both fields are localized in order to maximize the overlap.

Sub wavelength field localization can be achieved by excitation of localized surface plasmon polaritons.

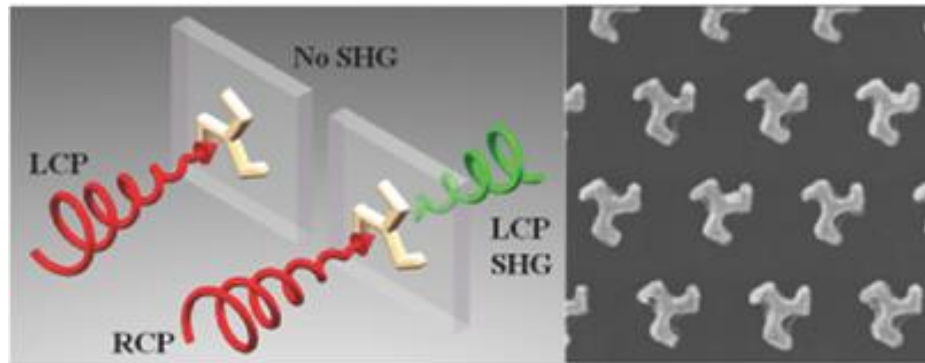


[Fisher and Martin, Opt. Express 16, 9144-9154 (2008)].

Renewed interest due to development of metamaterials and nanotechnologies

S. Chen et al.

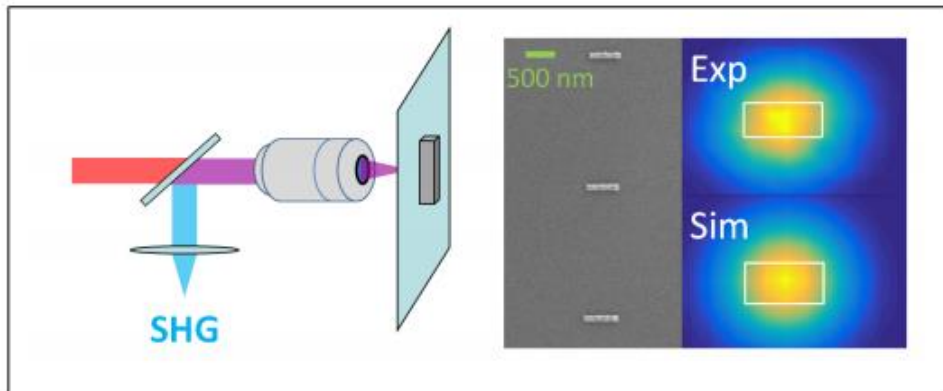
Adv. Mat. Vol 28, 15, pp 2992–2999, (2016)



M. Ethis de Corny et al.

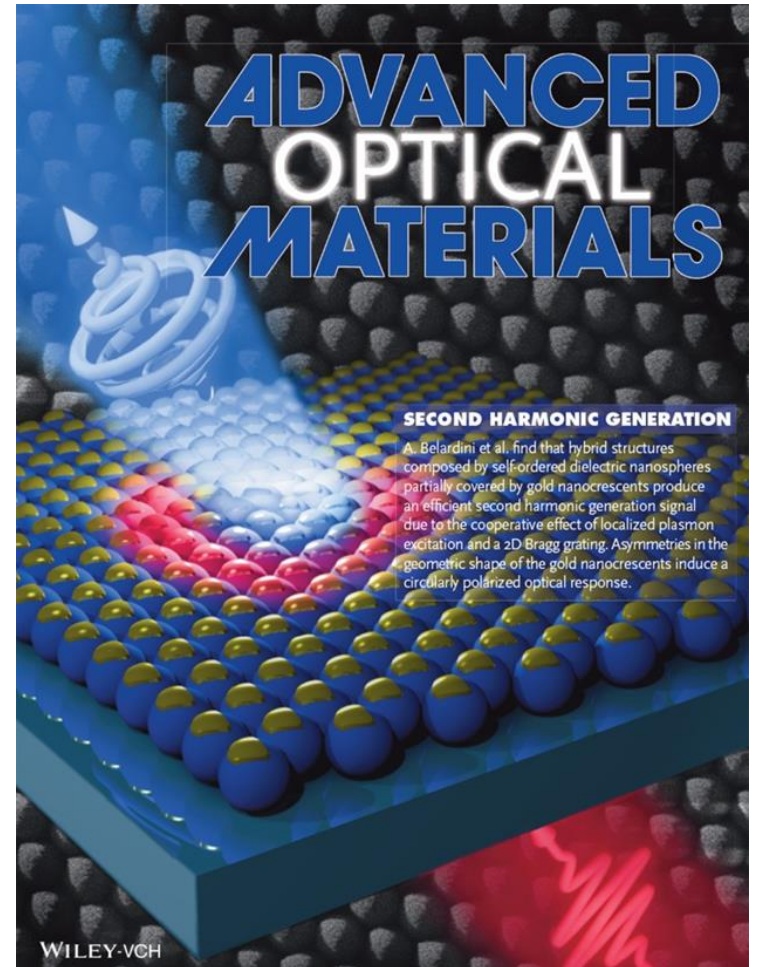
Just accepted ACS photonics Sept. 2016

Wave-mixing origin and optimization in single and compact aluminum nanoantennas.



A. Belardini et al.

B. Adv.Opt.Mat, Vol.2 Is.3, pp.208-213 (2014)



Linear and Nonlinear Optical Response of Metals

We begin by assuming that at optical frequencies the linear response of a metal is strongly affected by the bound valence electrons.

$$\varepsilon_r(\omega) = \varepsilon_D(\omega) + \sum_{j=1}^5 \frac{G_j \omega_p^2}{\omega_{0,j}^2 - \omega^2 - i\omega\kappa_j}$$

$$\varepsilon_D(\omega) = 1 - \frac{\omega_0^2}{\omega^2 - i\omega\kappa_0}$$

we model the optical response of the metal by assuming an effective current density:

$$\vec{J} = \vec{J}_D + \frac{\partial \vec{P}_{b.e.}}{\partial t}$$

At this stage we consider nonlinear effects related to the response of conduction electrons only.

Concerning second order nonlinear response we separate bulk and surface contributions

$$\vec{J}_{NL}^{Bulk} = -i2\omega \left[\gamma \delta' \left(\vec{E}_1 \cdot \vec{\nabla} \right) \vec{E}_1 + \gamma d \vec{\nabla} \left[\vec{E}_1 \cdot \vec{E}_1 \right] \right];$$

Bulk nonlinear term driven by absorption losses. It is not present in the classical free electron gas theory

$$\hat{X} \cdot \vec{J}_{NL}^{Surface} = -i2\omega (4\gamma b) E_{1,X}^{(-)} E_{1,Y}^{(-)} \delta(Y);$$

$$\hat{Y} \cdot \vec{J}_{NL}^{Surface} = -i2\omega (2\gamma a) \left[E_{1,Y}^{(-)} \right]^2 \delta(Y);$$

$$\hat{Z} \cdot \vec{J}_{NL}^{Surface} = -i2\omega (4\gamma b) E_{1,Z}^{(-)} E_{1,Y}^{(-)} \delta(Y);$$

$$d = \alpha\beta;$$

$$\delta' = 2\alpha\beta(\alpha - 1);$$

$$b = -\alpha^2\beta;$$

$$a = -\alpha^2\beta \frac{(\varepsilon_{r,\omega} + 3)}{2};$$

$$\alpha = \frac{\omega}{\omega + i\kappa_0};$$

$$\beta = \frac{2\omega}{2\omega + i\kappa_0};$$

$$\gamma = \frac{e\varepsilon_0\omega_0^2}{8m\omega^4}$$

A. Benedetti, M. Centini, C. Sibilia, M. Bertolotti, J. Opt. Soc. Am. B 27 3 408-416 (2010)

F. X. Wang, F. J. Rodríguez, W. M. Albers, R. Ahorinta, J. E. Sipe, and M. Kauranen, Phys. Rev. B 80, 233402 (2009)

Numerical evaluation of generated second harmonic field

The generated field pattern can be calculated by considering the equation for the generated SH electric field:

Being:

$$\left(\vec{\nabla} \wedge \vec{\nabla} \wedge - \frac{(2\omega)^2}{c^2} \bar{\bar{I}} \right) \vec{E}_2(\vec{r}) = i(2\omega) \mu_0 \vec{J}_2(\vec{r});$$

$$\vec{J}_2 = -i(\epsilon_{r,2} - 1)2\omega\epsilon_0 \vec{E}_2 + \vec{J}_{NL}^{Bulk} + \vec{J}_{NL}^{Surface};$$

The formal solution is:

$$\begin{aligned} \vec{E}_2(\vec{r}) = & \lim_{V_s \rightarrow 0} \int_{V-V_s} k_0^2 \chi_{b,2}(\vec{r}') \bar{\bar{G}}_E(\vec{r}, \vec{r}', 2\omega) \cdot \vec{E}_2(\vec{r}') d\vec{r}' - \bar{\bar{L}} \frac{\chi_{b,2}(\vec{r})}{\epsilon_{b,2}} \vec{E}_2(\vec{r}) + \\ & + i2\omega\mu_0 \lim_{V_s \rightarrow 0} \int_{V-V_s} \bar{\bar{G}}_E(\vec{r}, \vec{r}', 2\omega) \cdot \vec{J}_{NL}^{Bulk}(\vec{r}') d\vec{r}' - \frac{i}{2\omega\epsilon_0\epsilon_{b,2}} \bar{\bar{L}} \cdot \vec{J}_{NL}^{Bulk}(\vec{r}) + \\ & + i2\omega\mu_0 \int_V \bar{\bar{G}}_E(\vec{r}, \vec{r}', 2\omega) \cdot \vec{J}_{NL}^{Surface}(\vec{r}') d\vec{r}'; \end{aligned}$$

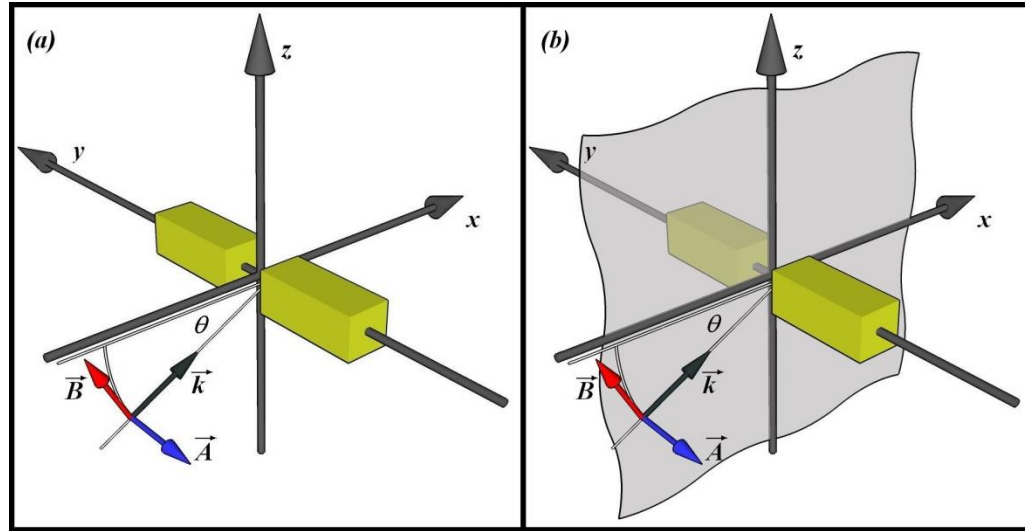
where the Green's tensor G is defined as:

$$\begin{aligned} \bar{\bar{G}}_E(\vec{r}, \vec{r}', 2\omega) &= \left[\bar{\bar{I}} + \frac{1}{k_b^2} \vec{\nabla} \vec{\nabla} \right] G_{0b} = \\ &= \frac{1}{4\pi} \left[\bar{\bar{I}} + \frac{1}{k_b^2} \vec{\nabla} \vec{\nabla} \right] \frac{e^{ik_b|\vec{r}-\vec{r}'|}}{|\vec{r}-\vec{r}'|}; \end{aligned}$$

G_{0b} is the 3D Green's scalar function for the SH frequency. V is the volume of the metallic scatterers.

**Integral equation is discretized and solved adapting a method detailed in:
O.J.F. Martin and N.B. Piller, Phys. Rev. E, Vol 58, 3 (1998)**

Numerical analysis: Linear properties

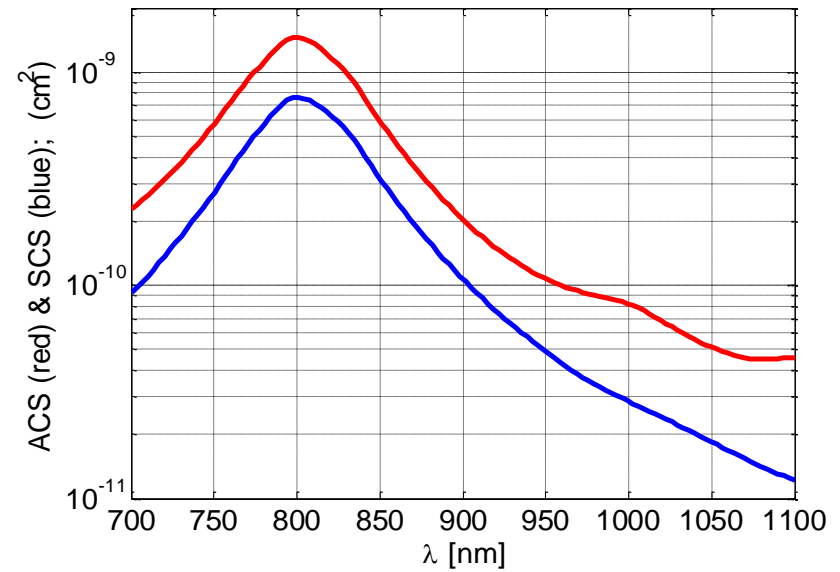


length of each element of the nanoantenna is 100 nm,
 gap between elements is 30 nm.
 Variable cross section thickness
 from (10 x 10) nm² to (36 x 36) nm².

$$ACS = \frac{-\int_S \text{Re}(\vec{E}_\omega \times \vec{H}_\omega^*) \cdot \hat{n} dS}{\text{Re}(\vec{E}_{0,\omega} \times \vec{H}_{0,\omega}^*)}$$

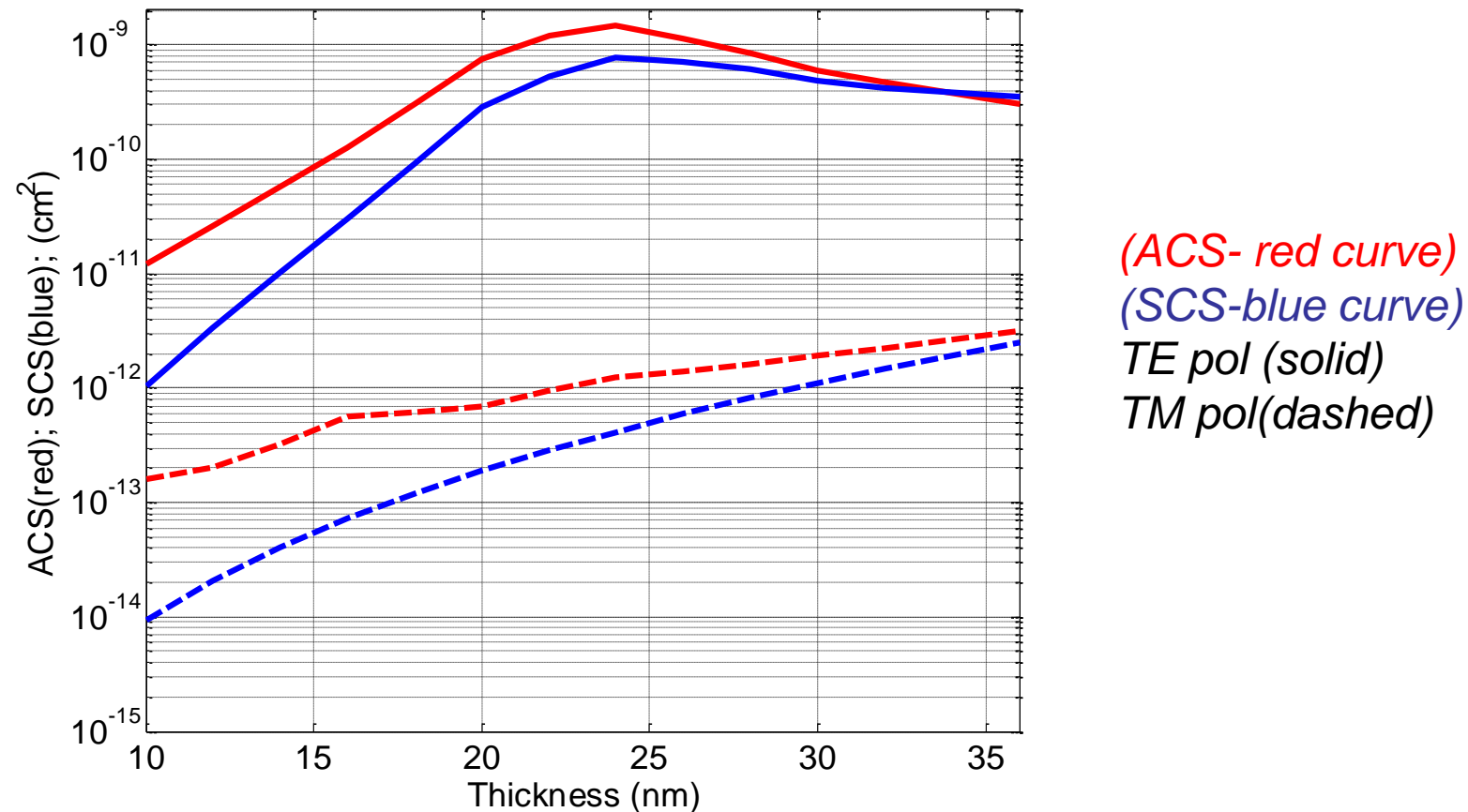
$$SCS = \frac{\int_S \text{Re}(\vec{E}_{SC,\omega} \times \vec{H}_{SC,\omega}^*) \cdot \hat{n} dS}{\text{Re}(\vec{E}_{0,\omega} \times \vec{H}_{0,\omega}^*)}$$

(24x24) nm² TE (y) pol

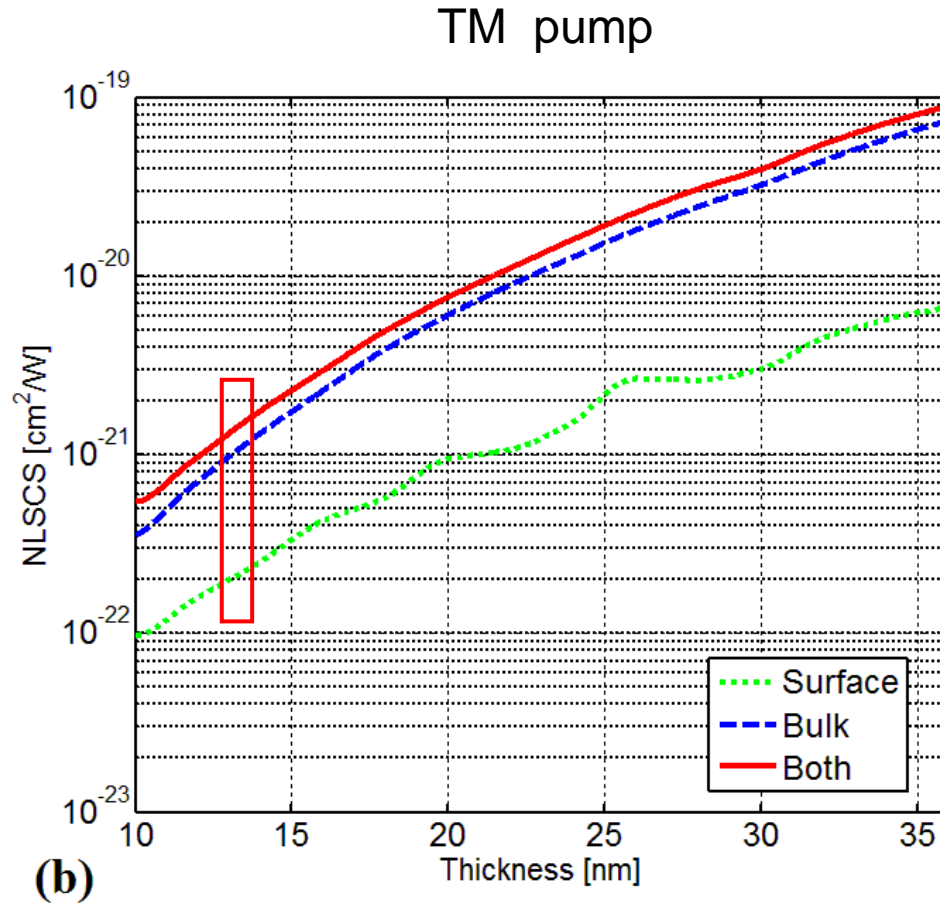


Numerical analysis: Linear properties

Different behavior between TE (y) and TM (z) polarization



Numerical analysis: Nonlinear properties

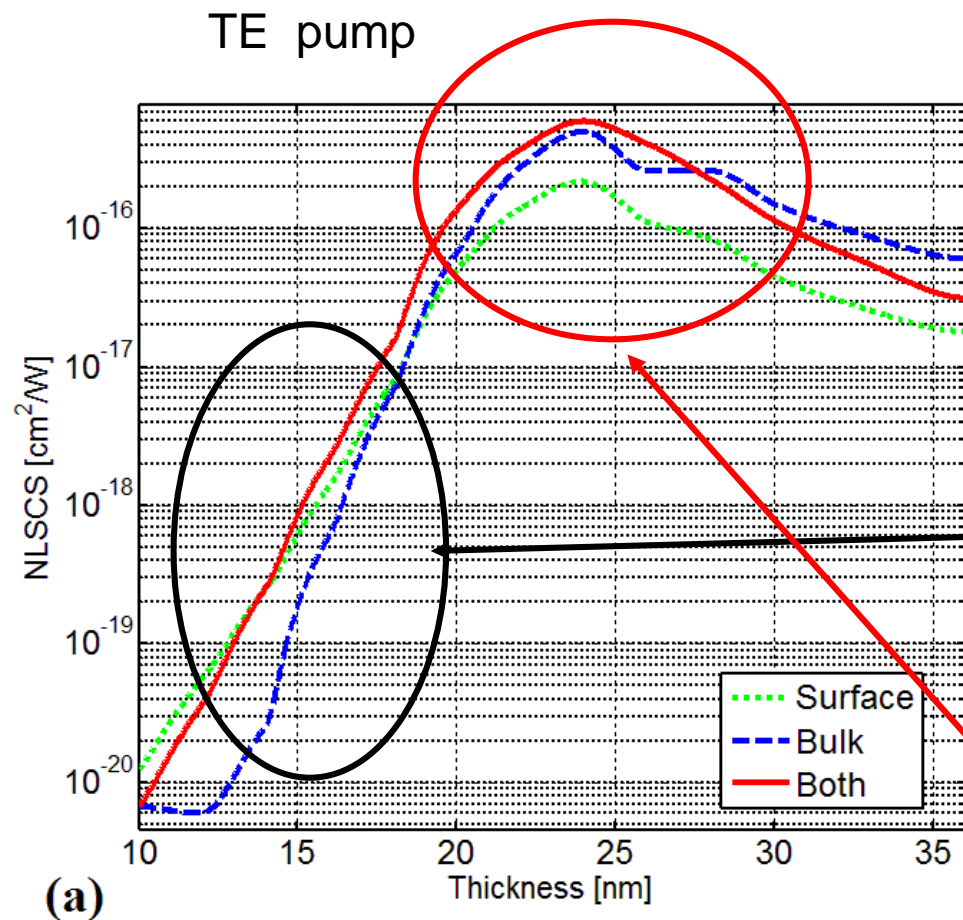


$$NLSCS = \int_S \sigma(\theta, \varphi) d\Omega;$$

$$\sigma(\theta, \varphi) = \frac{2S_{inc} \cdot \text{Re}(\vec{E}_{SC,2\omega} \times \vec{H}_{SC,2\omega}^*) \cdot \hat{n} \cdot R^2}{P_{0,\omega}^2};$$

For TM pump, there are negligible effects due to field localization because the antenna is out of resonance. The SH signal is mostly generated by bulk contributions.

Numerical analysis: Nonlinear properties



the linear response of the system is stronger with respect to the TM case. High localization of the pump field at metal/air interfaces, higher absorption means higher field penetration inside the metal.

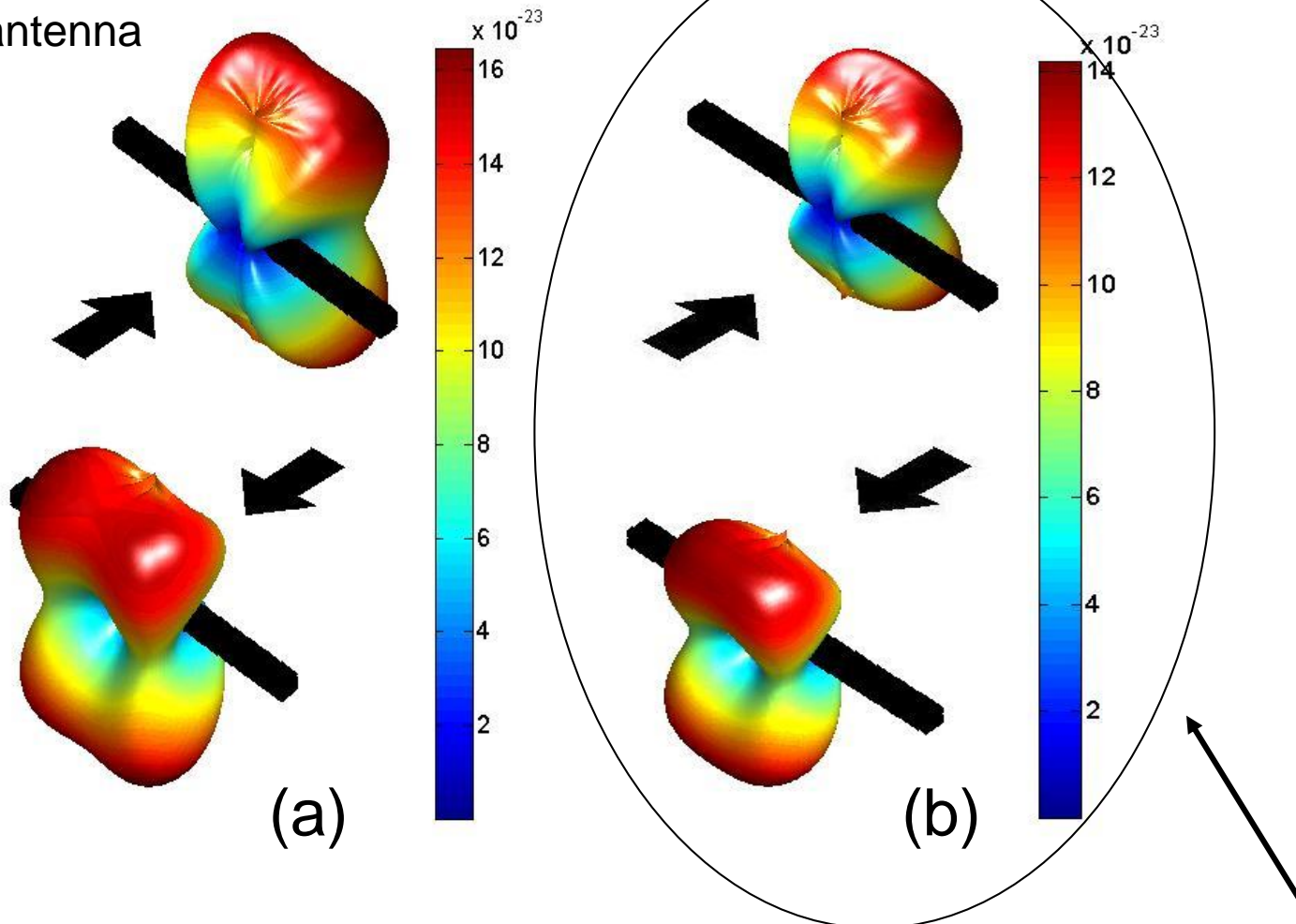
Surface contributions are stronger.

Pump field becomes more localized close to the air gap between the two rods and at the antenna's tips, reducing the amount of surface effectively contributing to the process and enhancing the bulk nonlinear response.

Numerical analysis: Far field pattern

Second harmonic differential scattering cross section [cm^2/W] for TM pump

(13x13) nm^2 antenna



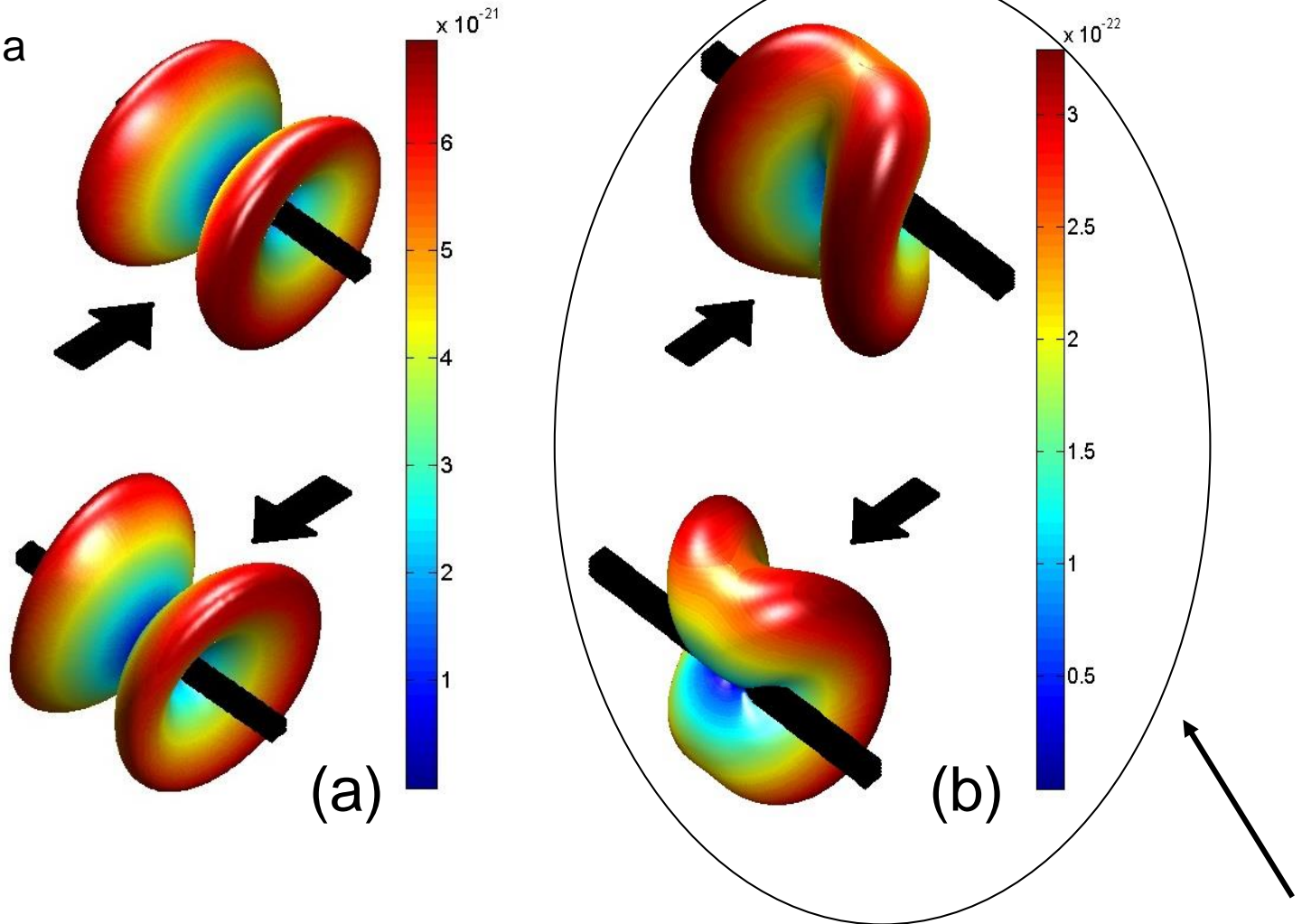
Surface terms can be neglected. Measured signal can be considered only coming from bulk contributions

Only bulk nonlinear contributions

Numerical analysis: Far field pattern

Second harmonic differential scattering cross section [cm^2/W] for TE pump

(13x13) nm^2 antenna

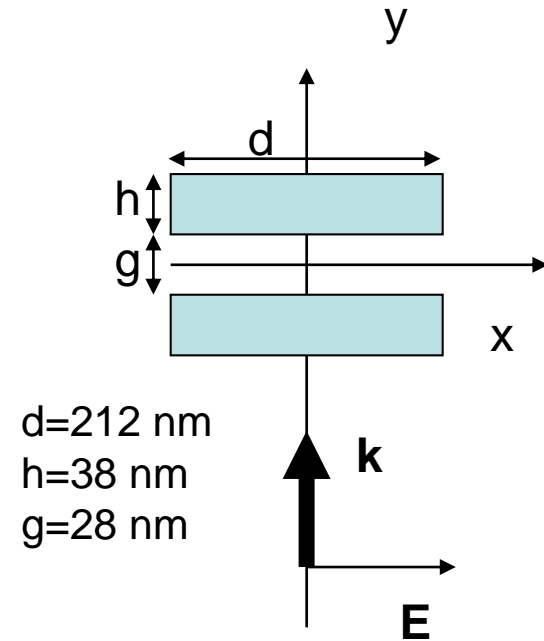
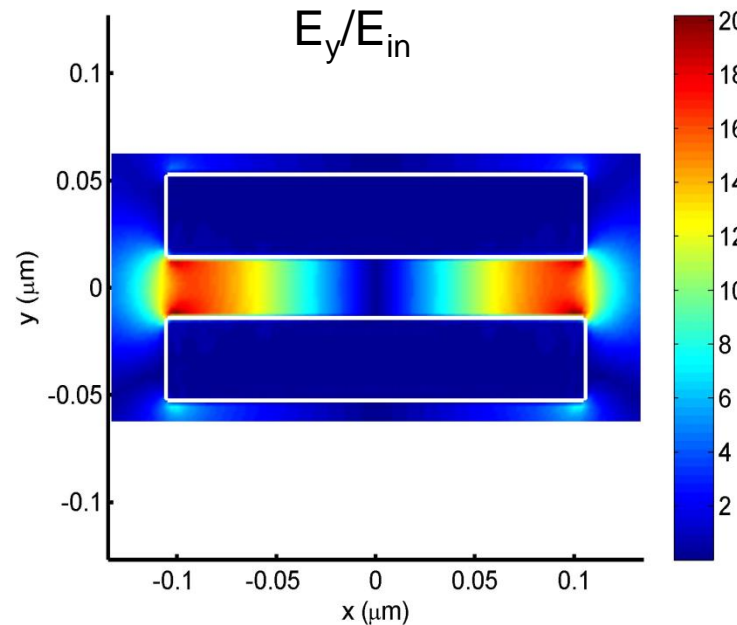
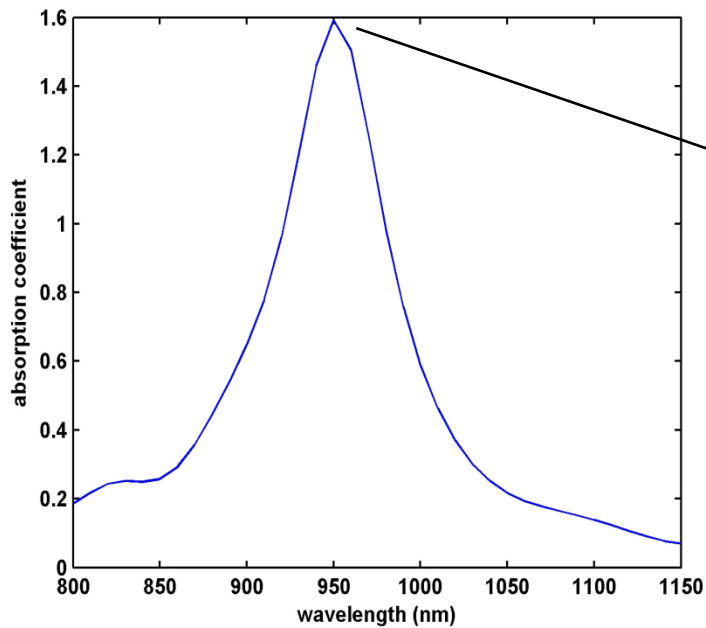


Only bulk nonlinear contributions

Silver Coupled Resonators

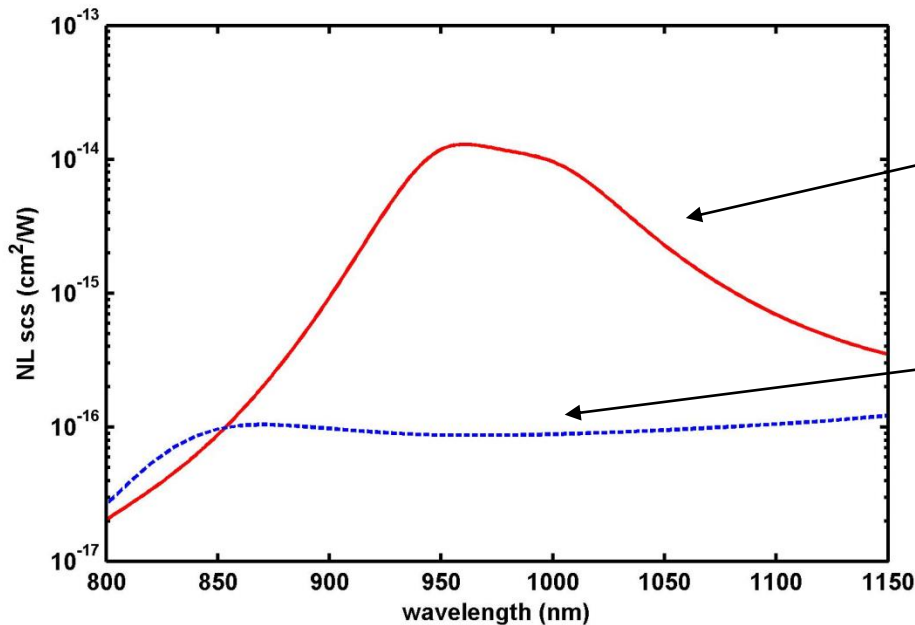
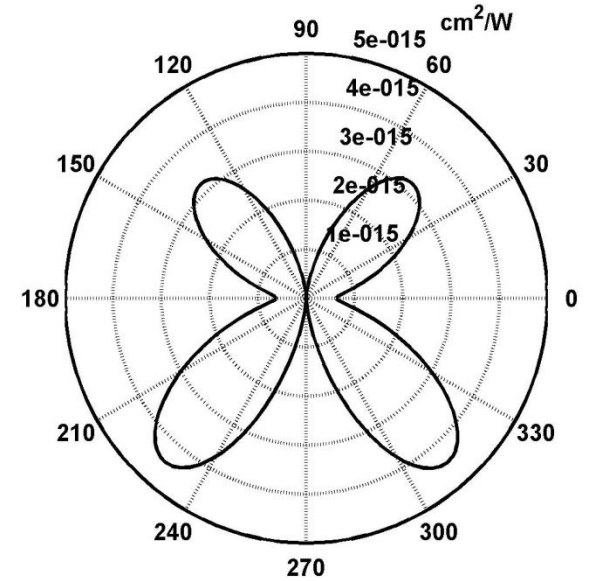
Efficiency factor for absorption at the FF field:

$$Q_{abs} = -\frac{2}{P_{in}} \operatorname{Re} \int_S (\vec{E} \times \vec{H}^*) \cdot \hat{n} dS = -\frac{2R}{I_{in} d} \operatorname{Re} \int_0^{2\pi} (\vec{E} \times \vec{H}^*)_{\hat{n}} d\theta;$$



Silver Coupled Resonators

Enhanced second harmonic non linear scattering cross section due to resonant excitation of a localized surface plasmon polariton in the nanoresonator.

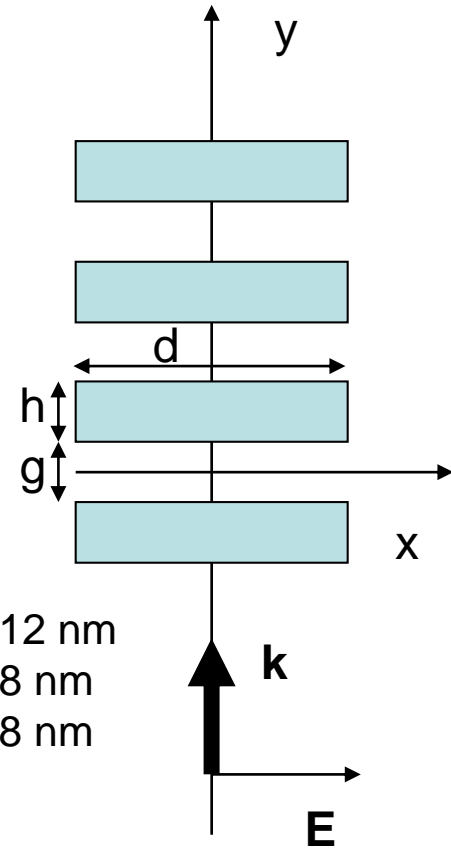
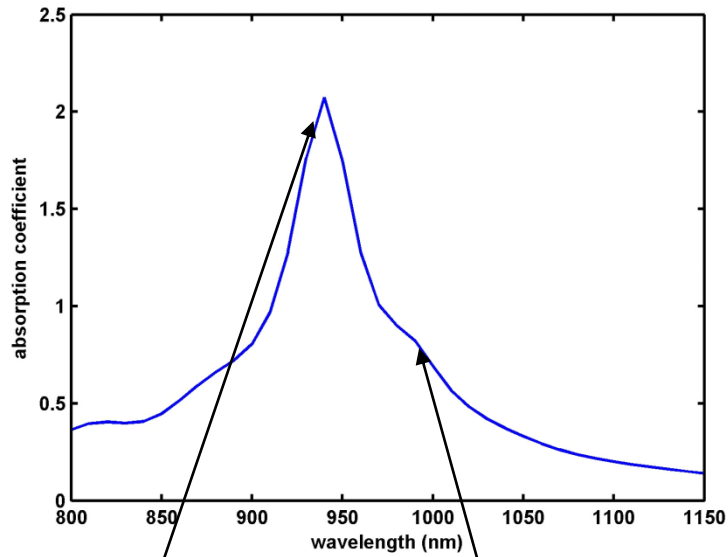


Two-rod nanoresonator

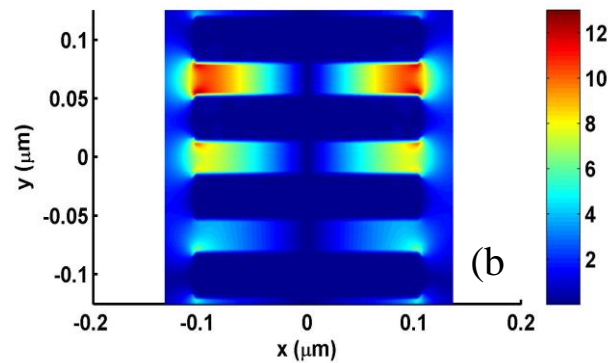
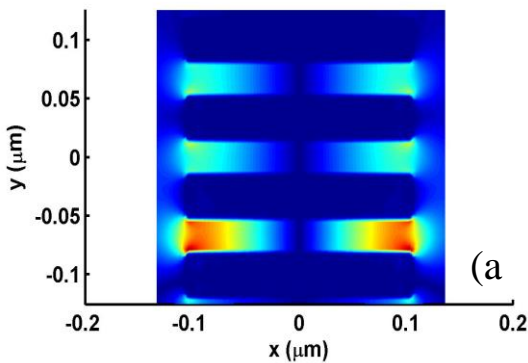
Single rod

Silver Coupled Resonators

FF

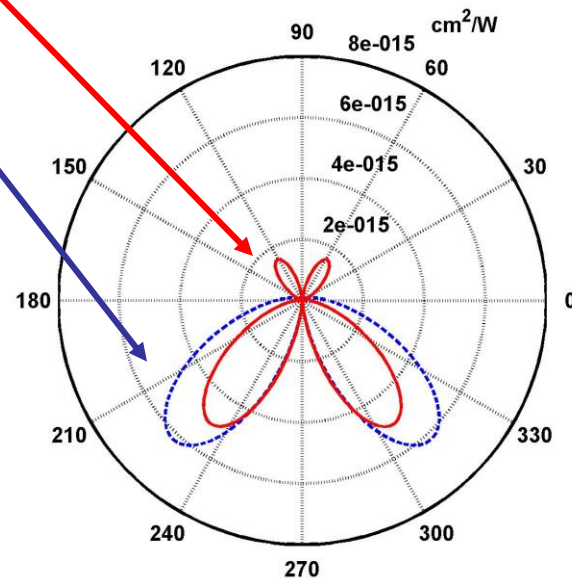
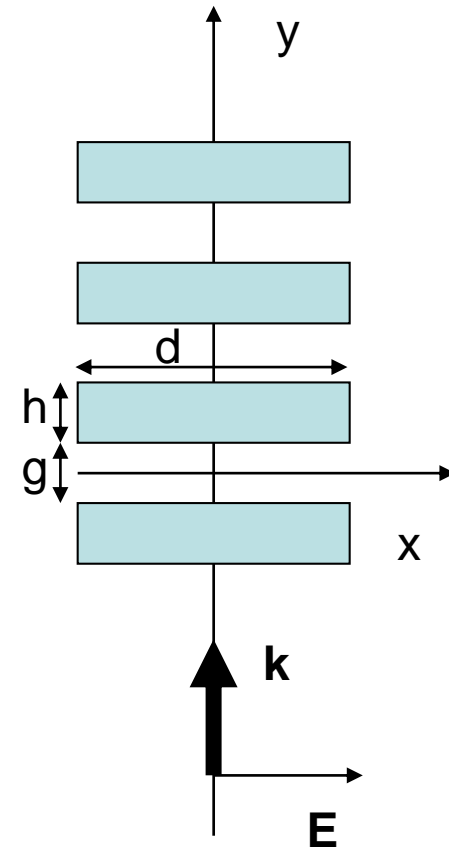
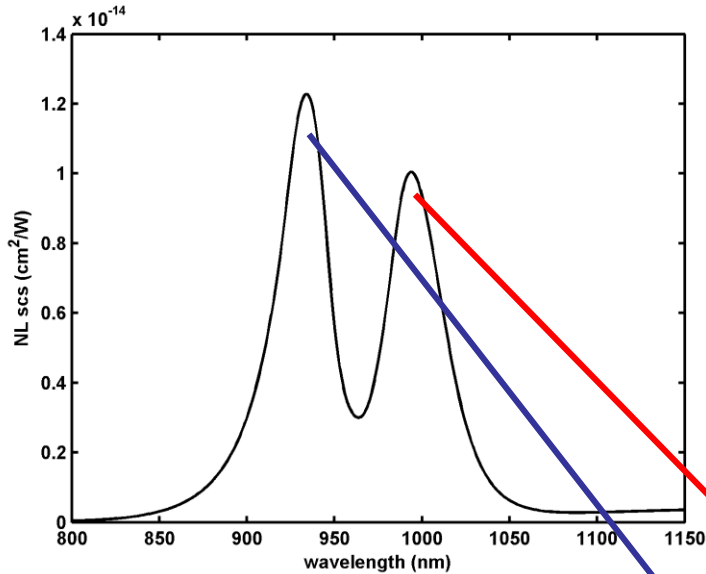


$d=212$ nm
 $h=38$ nm
 $g=28$ nm



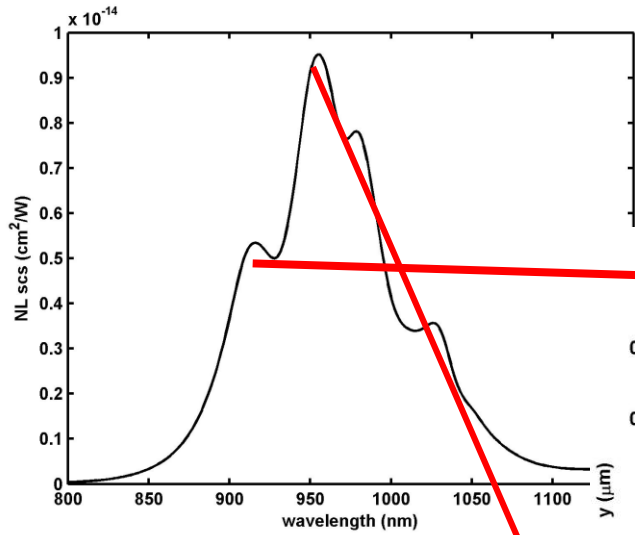
Silver Coupled Resonators

SH

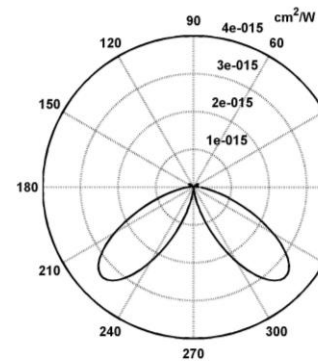
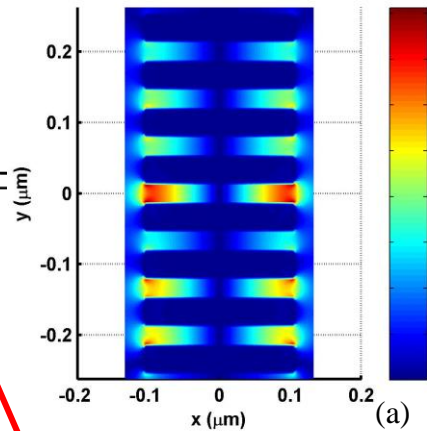


SH far field pattern contains information of the FF sub-wavelength localization properties: Different FF nearfield profiles produce different SH emission patterns.

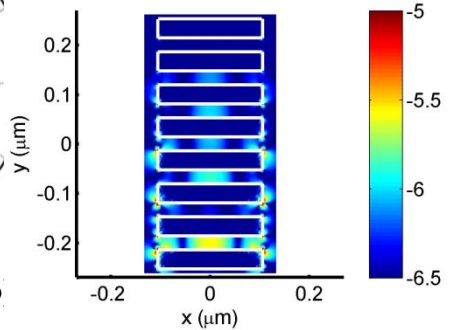
Silver Coupled Resonators



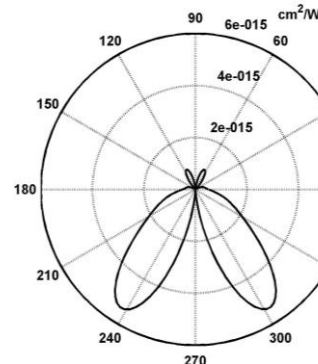
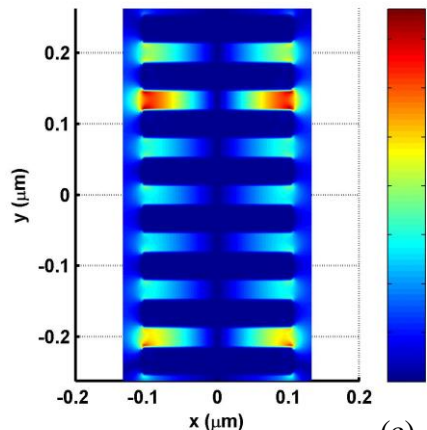
FF @ 920 nm



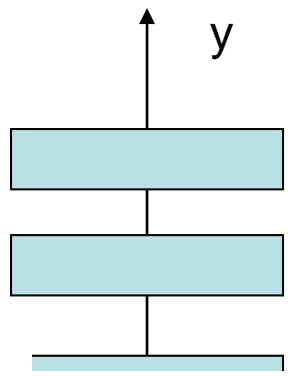
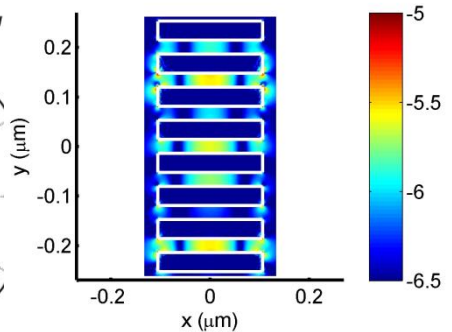
(b)



FF @ 960 nm

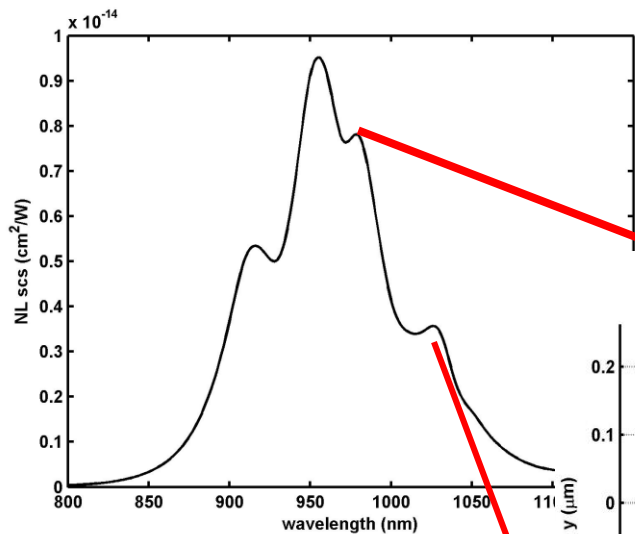


(d)

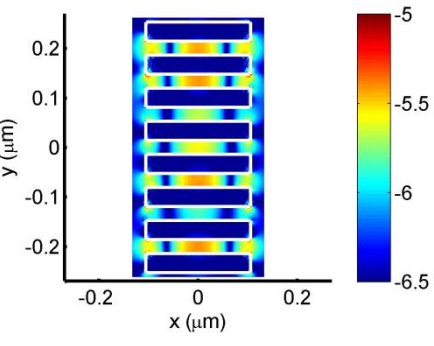
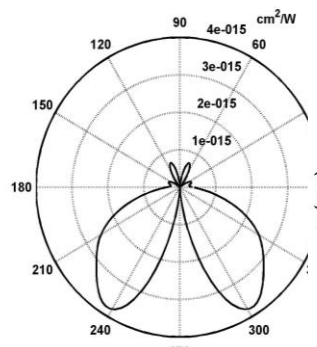
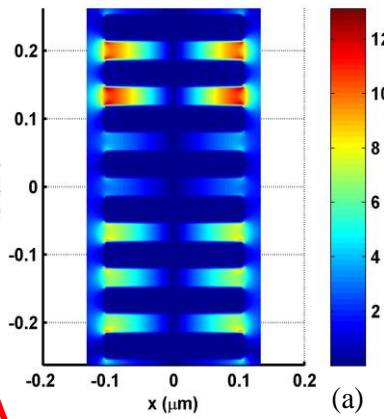


E

Silver Coupled Resonators

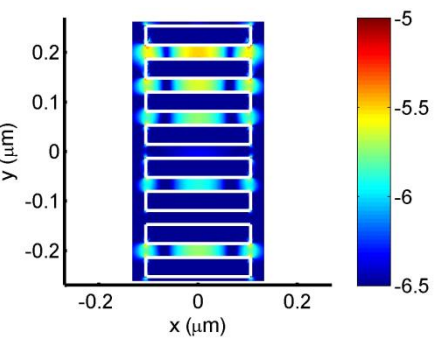
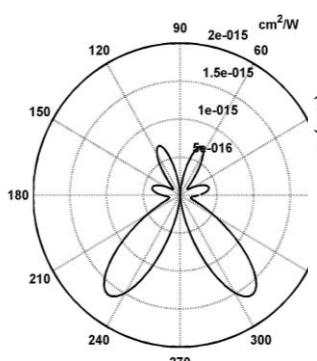
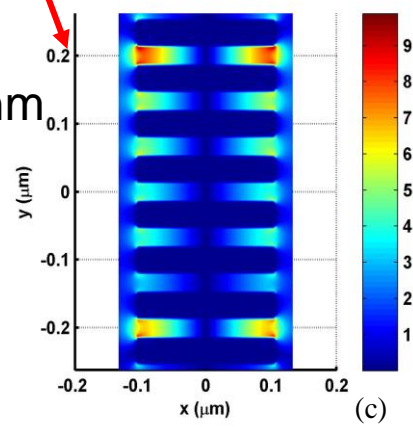


FF @ 980 nm

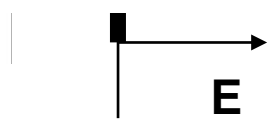
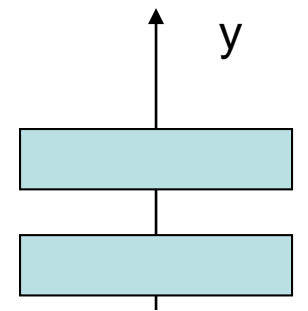


(b)

FF @ 1030 nm



(d)



CONCLUSIONS

For nanoscaled metal structures the nonlinear surface contributions strongly reduce their relative weight in the overall SHG with respect to bulk contributions.

A variety of cases can be obtained: great attention must be paid when neglecting the nonlinear surface sources in numerical models of SHG, because, every case must be considered by itself, without performing a priori simplification.

Second harmonic emission pattern of coupled nanoresonators ensembles can be tailored by changing shapes and distance between the elements.

Near field and far field properties of the generated second harmonic are strictly related to localization properties of the pump field. The main angle of emission changes as a function of the pump frequency.

Further optimization of the proposed geometries might lead to applications for sensors and nano sources for single molecule fluorescence.

Thanks to...

Concita Sibilìa

Mario Bertolotti

Alessandro Belardini

SBAI, Sapienza Università di Roma

Alessio Benedetti

DIET, Sapienza Università di Roma

...and thank you for the attention!